*Annu. Rev. Earth Planet. Sci. 1993. 21:525–55*


# IMPACT EROSION OF TERRESTRIAL PLANETARY ATMOSPHERES

*Thomas J. Ahrens*

Lindhurst Laboratory of Experimental Geophysics, Seismological Laboratory 252-21, California Institute of Technology, Pasadena, California 91125

KEY WORDS: atmospheric escape, atmospheric loss, earth accretion, early atmosphere



## 1. INTRODUCTION

The idea that planetary atmospheres can erode as a result of impact, and thus lose mass along with solid and molten high velocity ejecta during accretional infall of planetesimals follows from such early thoughtful works as that of Arrhenius et al (1974), Benlow & Meadows (1977), Ringwood (1979), and Cameron (1983). Ahrens et al (1989) describe how planetary impact accretion (and impact erosion) concepts lead naturally, from the idea that atmospheres form and erode during planetary growth.

The theory of planetary system formation from a disc of gas, and later, gas and dust, corotating around a proto-sun, which evolves into increasingly larger planetesimals, is described by Safronov (1969), Wetherill (1980, 1990), and Kaula (1979) (Figure 1). In this model, planets grow as a result of mutual attraction and collision of planetesimals within a solar nebula which evolved from the primordial disc. An important step in the wide acceptance of this model is the demonstration that the requirement of planetesimals with diameters $>10$ m will form from a dust and gas mixture before the nebular gas is removed from the terrestrial planet region in $\sim 10^6$ years (Weidenschilling 1988, 1989). Recently, very strong support for the early phase of the Safronov-Wetherill-Kaula scenario of planetary growth from a gaseous and possibly dusty disc of planetesimals, has come



0084–6597/93/0515–0525$02.00

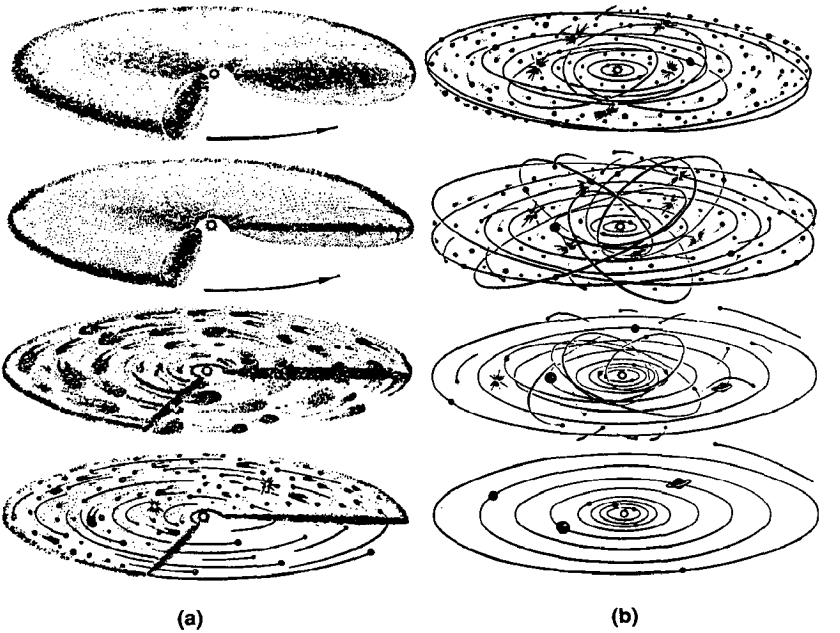


*Figure 1* The solar system via the Safronov-Wetherill-Kaula scenario. (*a*) Formation of asteroid-size intermediate bodies form the dust component of the solar nebula. (*b*) Runaway accretion to intermediate-sized bodies. Impact accretion of intermediate-sized bodies into planets. Accretion of gas by giant planets is not shown. The initially flat system of intermediate bodies thickens due to their mutual gravitational perturbations. (After Levin 1972.)

from discovery using infrared, optical, and radio imagery of disc-shaped circumstellar gas and dust clouds around T-Tauri stars (e.g. HL Tauri and R Monocerotis) (Beckwith et al 1986, Sargent & Beckwith 1987) and main sequence stars (e.g. $\beta$-Pictoris) (Smith & Terrile 1984) (Figure 2). Although the gaseous rotating discs around T-Tauri stars have been imaged via microwave radio interferometry and infrared techniques, it has not yet been demonstrated that these discs contain accreting planetesimals. Recent observations of the $^{13}CO$ emission spectra and the blackbody thermal emission from the circumstellar gas disc around HL Tauri indicate that this disc extends out to a radius of 2000 AU, but is less than 380 AU thick (where 1 AU is the Earth-Sun distance $= 1.5 \times 10^8$ km). Moreover, the spectra are consistent with the gas and dust moving in bound orbits around this star (Sargent & Beckwith 1992).

Here I review current ideas about the nature of the planetesimals—composition, size distribution, and the planetary encounter velocity. Pre-

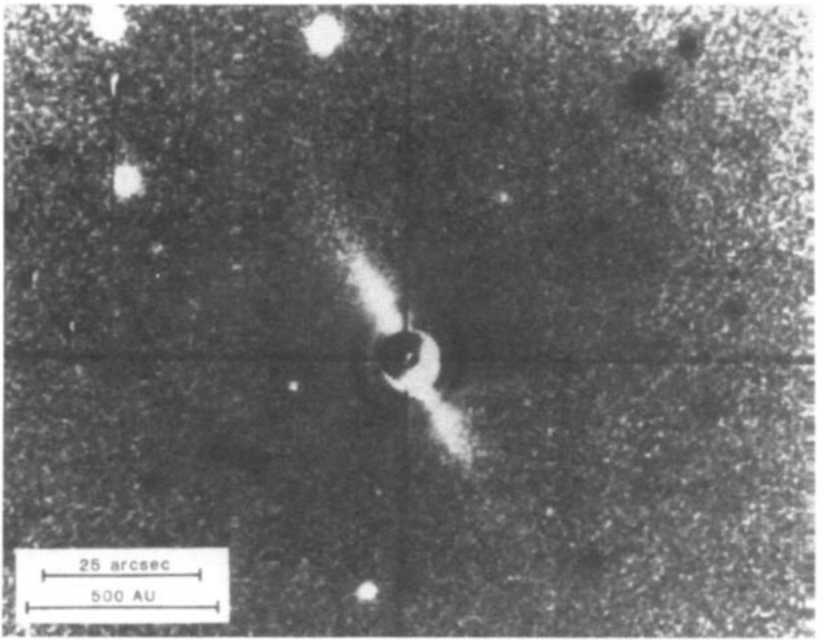


*Figure 2* Enhanced image of the star $\beta$-Pictoris demonstrates what appears to be the beginnings of another solar system. The disc of material surrounding $\beta$-Pictoris extends $60 \times 10^9$ km from the star, which is located behind a circular occulting mask in the center of the image. The disc material is probably composed of gases and grains of ices, carbonaceous chondrite-like organic substances, and silicates. These are the materials from which the comets, asteroids, and planets of our own solar system are thought to have formed. (After Smith & Terrile 1984.)

vious papers on accretion and erosion of planetary atmospheres as a result of multiple impacts are also reviewed. Finally, the effects of blowing off a substantial fraction of the atmosphere from a terrestrial planet due to a single giant body impact are discussed.

## 2. PLANET FORMING MATERIALS

The planets and minor objects in the solar system appear to have accreted from the following three components:

1. Planetesimals similar to meteorites.

   The constitution of the terrestrial planets suggests that they accreted largely from planetesimals with a range of composition including primitive objects, such as C1 chondrites, as well as objects similar to differ-

entiated metal and silicate meteorites. The linear relation in Figure 3 indicates how similar the major element composition of the chondritic meteorites are to the Sun. It is presumed that these objects are similar in bulk chemistry to some of the planet-forming planetesimals. This concept is reinforced by Figure 4, which illustrates that the noble gas abundance patterns of terrestrial planets are similar to each other and to primitive meteorites such as C1 chondrites. Meteorites are often taken to be typical of the planetesimals existing within the inner zone of the solar nebula from which the terrestrial planets accreted. The vestiges of the planetesimals of the inner solar system are believed to be the asteroids. We presumably sample these objects via meteorites that fall on the Earth. Some of the planetesimals that formed the terrestrial planets were also probably similar in composition to the



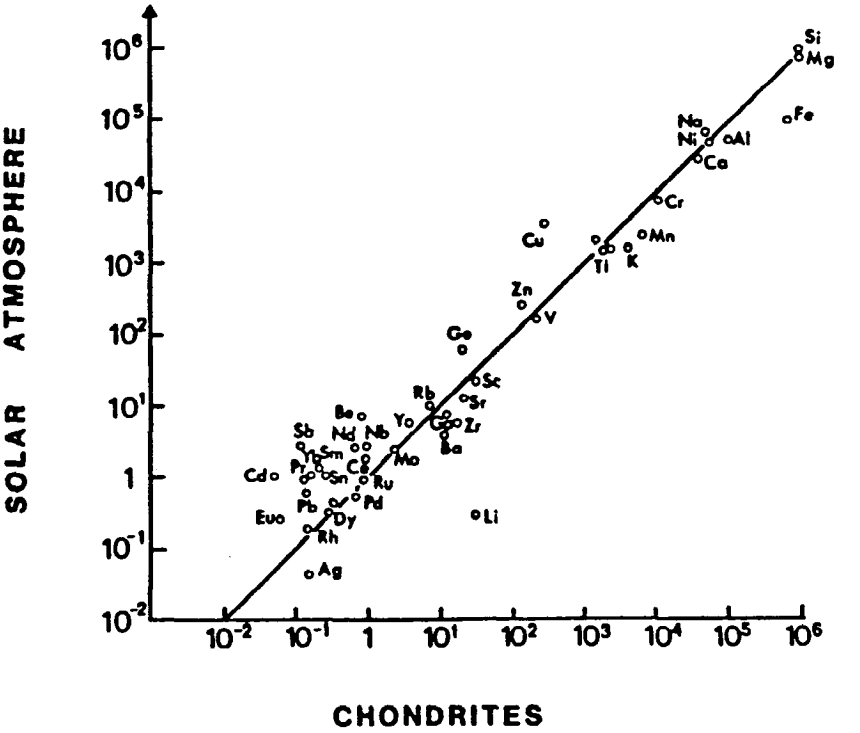


*Figure 3* Atomic abundance of the elements in the solar photosphere vs the abundance in chondritic meteorites. Plot is normalized with respect to $10^6$ atoms of Si. (After Allègre 1982.)

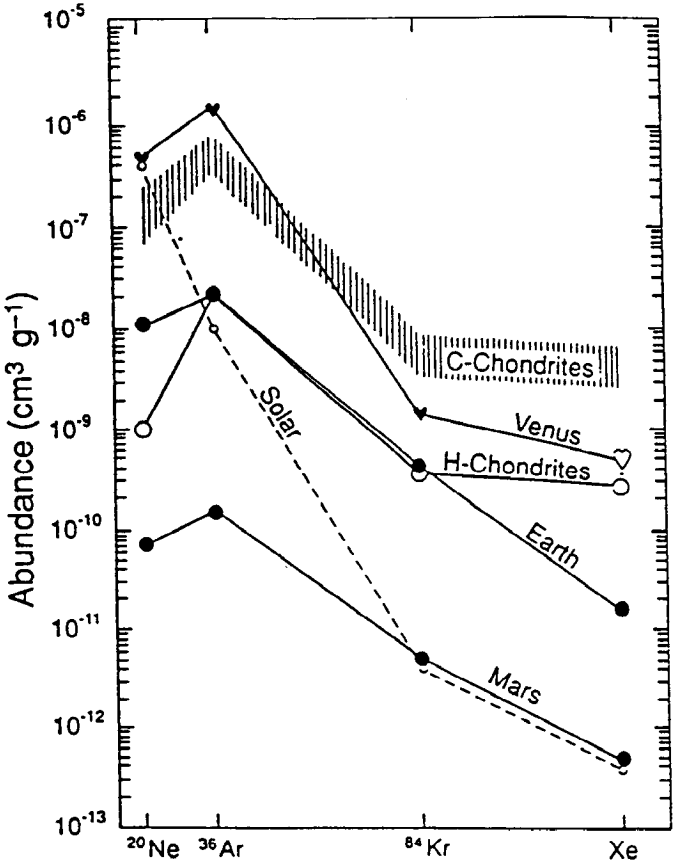


*Figure 4* Abundances of noble gases in planetary atmospheres and chondritic meteorites given as cubic centimeters per gram of rock. [After E. Anders, personal communication in Owen et al (1992).]

present comets. Largely because of the gravitational perturbation from passing stars in the Galaxy, comets are perturbed from their orbits in the Oort cloud (which is spherically concentric with the Sun) at a radius of $10^4$ to $10^5$ AU, and possibly via the Kuiper belt (Duncan et al 1988) can achieve highly eccentric orbits which, near perihelion, result in collision with the terrestrial planets. The large masses of Jupiter and Saturn also play an important role in perturbation of cometary orbits, once these objects enter the planetary zone. Shoemaker et al (1990)

estimated that some 30% of the recent impactor flux on the Earth may be cometary. How much of this flux has provided the volatile budgets of the terrestrial planets is presently unclear (e.g. Grinspoon & Lewis 1988 and Donahue & Hodges 1992) because of the similarity of the cometary nonvolatile major element inventory with that of the C1 chondrites (Jessberger et al 1989).

2. Cometary planetesimals.

   In contrast to the silicate and iron-rich planetesimals, the planetesimals that made up the cores of the giant outer planets—Jupiter and Saturn, and to a lesser degree Neptune and Uranus, and possibly Pluto—were ice-rich. In analogy to the terrestrial planets whose planetesimals are probably related to the main belt asteroids, the remnants of the planetesimal swarm that formed the icy and silicate cores of the giant planets are now associated with comets. The generally smaller size ($<10$ km diameter) of the comets (relative to asteroids) suggests that in the outer solar system the density of matter in the solar nebula was never great enough for the ice-rich planetesimals to experience substantial mutual gravitational attraction, resulting in impact accretion.

3. Solar nebulae gas.

   In contrast to terrestrial planets, Jupiter and Saturn, and to a lesser degree Uranus and Neptune, appear to have gravitationally captured large quantities of solar nebular gases, after building up their initial planetary core from ice, silicate, and carbon-rich objects. The large planets thus retain a large solar-like reservoir of $H_2$ and He. Pollack & Bodenheimer (1989) suggested that the ratio of carbon to hydrogen in the atmospheres (which dramatically increases in the order: Jupiter, Saturn, Uranus, and Neptune) directly reflects a decreasing budget of accreted solar nebular hydrogen.

## 3. TERRESTRIAL PLANETARY VOLATILES

On the basis of the general similarity of the noble gas abundances of the terrestrial planet atmospheres to the noble gas component that was processed within planetesimals before their accretion, I infer that terrestrial planet atmospheres originated from planetesimals similar to primitive meteorites. Cometary-like planetesimals may have also contributed to the terrestrial planet volatile inventory. Notably, the thermal and gravitational evolution of the planets are distinctly different; however, their relative noble gas inventories are similar. The solid phases containing noble gases presumably are still present in the asteroids and demonstratively occur in meteorites. Small meteorites impact at sufficiently slow terminal velocity

that the noble gases are not released upon impact. They still contain the complement of noble gases present 4.6 Gyr ago prior to the planet-forming epoch (Figure 1). The planetesimal origin of noble gases in planetary atmospheres is also indicated by the observation that the two key mass-selective, gas-loss mechanisms (e.g. Hunten et al 1989) for atmospheric escape—Jeans loss and hydrodynamic escape—predict abundance patterns, starting from a solar (noble gas) pattern, that are quite different from those in the atmospheres of Mars, Earth, and Venus.

## 4. SIZE DISTRIBUTION OF PLANETESIMALS

In Safronov's (1969) theory of planetary accretion, a simple power law distribution of the differential number of objects, $n(m)dm$, which occurs in a mass range $dm$ is assumed:

$$n(m) = [N_0 \exp(-m/m_0)]/m_0, \tag{1}$$

where $n(m)dm$ is the number density of objects with mass between $m$ and $m+dm$, $N_0$ is the initial number density of objects, and $m_0$ is the mean mass of the body distribution. Wetherill (1990) showed that in previous "smooth" growth descriptions of accreting objects (e.g. Safronov 1969), the increase of mass, $dM/dt$, could be described by

$$\frac{dM}{dt} = \pi R^2 \bar{V}_{\text{rel}} \rho \left(1 + \frac{8}{3}\frac{\pi \rho_p R^2}{\bar{V}_{\text{rel}}^2}\right), \tag{2}$$

where $\bar{V}_{\text{rel}}$ is the average relative velocity between the large (accreting) objects (of density $\rho_p$ and radius $R$) and the nearby small objects (to be accreted), and $\rho$ is the small body mass density in space. Equation 2 can be written as

$$dM/dt = kR^q \tag{3}$$

where $k$ is a constant. When $\bar{V}_{\text{rel}}$ is large compared to the escape velocity from the large accreting object ($V_e$), $q \sim 2$. When $\bar{V}_{\text{rel}} \ll V_e$, $q \sim 4$. Initially smooth accretion models (Nakagawa et al 1983, Safronov 1969) used a constant intermediate value of $q = 3$. Moreover, recent modeling (Stewart & Kaula 1980, Stewart & Wetherill 1988) demonstrated that in swarms of unequal mass objects in an accreting disc, the mutual gravitational perturbations which result increase the mean velocities (essentially, $\bar{V}_{\text{rel}}$) of the smaller objects, such that the effective value of $q$ in Equation 3 increases from $\sim 2$ to $\sim 4$. As a result, a phenomenon termed "runaway growth" occurs as a result of the marginally larger objects growing rapidly at the expense of their smaller neighbors. At 1 AU, smooth growth from

$10^{20}$ gram objects to $10^{24}$ gram objects occurs in $\sim 10^4$ years, then a runaway growth occurs in an $\sim 10^5$ year period. Much of the proto-solar system mass ends up in $10^{26}$ gram (lunar to Mars size) proto-planets. Accretion of such large proto-planets gives rise to large body impacts during the latter stages of accretion.

## 5. PLANETESIMAL IMPACT VELOCITIES

As shown in Figure 1, the major element of motion of the planetesimals in ideal circular Keplerian circular orbits around the Sun is velocity ($v_s$), which, in the solar reference frame, is given by

$$v_s = \sqrt{GM_\odot/r}, \tag{4}$$

where $G$ is the gravitational constant ($6.67 \times 10^{-8}$ dyn-cm$^2$/g$^2$ or $6.7 \times 10^{-11}$ nm$^2$/kg$^2$), $M_\odot$ is the solar mass, and $r$ is the distance of the planetesimal from the Sun's center. Even for perfectly circular planar orbits, two objects at slightly different solar distances, initially will differ in velocity. Hence, the object closest to the Sun, $m_1$, will move in at a slightly higher speed, passing an object, $m_2$, which is further from the Sun. Gravitational interaction occurs in this two-body encounter, such that the object $m_1$ will experience a radial velocity increase given by

$$\delta v = m_2 v_s/(m_1 + m_2)E. \tag{5}$$

Here, $E$ is an encounter parameter which depends on the geometry and the relative masses of the objects. Continual gravitational interaction of adjacent objects gives rise to increasing orbital eccentricities, as well as inclination of the orbits. These in turn give rise to collisions which tend to damp out the velocity and orbital perturbations such as described by Equation 5. On average, for planetesimals relative to one another in orbit in a corotating disc of particles, their encounter velocities will be $v_\infty$. Safronov pointed out that the largest particles with an escape velocity, $v_e$, will have encounter velocities:

$$v_\infty = v_e/\sqrt{2\theta}. \tag{6}$$

Here the local escape velocity is

$$v_e = \sqrt{2Gm_p/R_p} = \sqrt{2R_p g}, \tag{7}$$

where $m_p$ is the mass of the largest planetesimal in a region, $R_p$ is the largest planetesimal radius, and $g$ is its gravitational acceleration. Here, $\theta$, the Safronov parameter, is usually taken to be about 4 or 5. The result

depends critically on $q < 2$. Otherwise, $v_\infty$ will be drastically reduced by multiple encounters with the smallest particles.

The impact velocity of a planetesimal is therefore

$$v_i = \sqrt{(v_e^2 + v_\infty^2)}. \quad (8)$$

Equation 8 implies that as planets grow by accretion, the planetesimal impact velocity is always somewhat greater than the planetary escape velocity. Moreover, Equation 2 indicates that as planets grow, so does the mass of the planetesimals which impact their surface. Both runaway growth and velocity of impact considerations have led to efforts to understand the essential physics of large-body impacts on the terrestrial planets by Benz et al (1989, 1986, 1987, 1988) and Kipp & Melosh (1986).

## 6. COACCRETION OF PLANETARY ATMOSPHERES

Although Lange & Ahrens (1982b) suggested that the impact-induced dehydration of water-bearing minerals in planetesimals such as serpentine $Mg_3Si_2O_5(OH)_4$ would produce a largely water-rich atmosphere on the growing planets, it was Abe & Matsui (1985) who first suggested the possibility that water in this atmosphere, and possibly the dust produced by planetesimal impact, could drastically alter the thermal regime on the surface of growing planets (Figure 5). They assumed that serpentine in planetesimals brought the Earth and the other terrestrial planets their

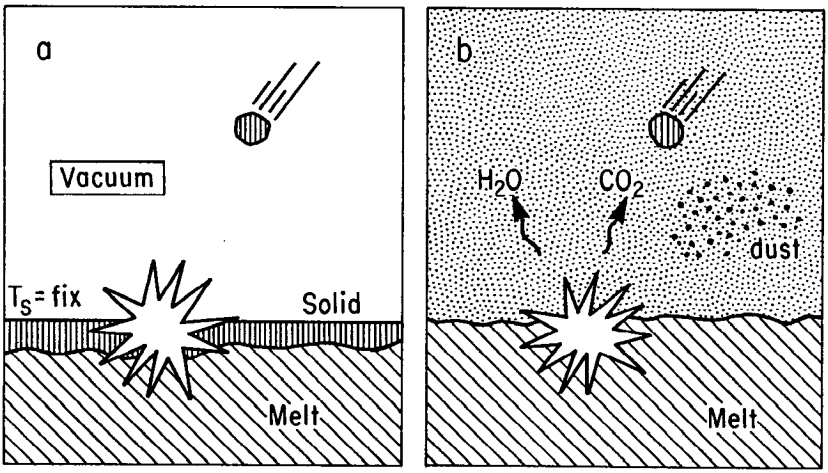


*Figure 5* Cartoon indicating the difference between the thermal regime of accretion via (*a*) previous studies and (*b*) "thermal blanketing." [Figure from Abe & Matsui (1985).]

water inventory during their accretion. Once impact pressures of infalling planetesimals exceeded $P \simeq 23$ GPa (for a porous regolith), the supply of water to the atmosphere was assumed to begin. Abe & Matsui (1985) estimated the peak shock pressure by

$$P = \rho_0[C_0 + (K' + 1)v_i/8]v_i/2, \tag{9}$$

where $\rho_0$ and $C_0$ are impacting planetesimal initial density and zero-pressure bulk sound velocity, respectively, and $K'$ is the partial derivative of the bulk modulus with respect to pressure. In these atmospheric accretion models the shock pressure is assumed to act on the entire impacting planetesimal and $H_2O$ is released, as well as lesser amounts of $CO_2$, $NH_3$, $SO_2$, and other volatiles present in primitive meteorites (e.g. C1 carbonaceous chondrites). Previous calculations have also included contributions to the atmosphere induced by shock-loading of volatiles already present in the material of the planetary surface layer (e.g. Lange & Ahrens 1982a).

Using the experimental value of 23 GPa as the shock pressure required to induce complete water loss for serpentine, Lange & Ahrens (1982b) and Abe & Matsui (1986) concluded that once the radius of the Earth reached between 0.2 to 0.4 of the present value ($R_\oplus$), thermal blanketing of the Earth caused by a dense water atmosphere occurred. Matsui & Abe (1986a) point out that thermal blanketing is a more severe condition than the greenhouse effect. In a greenhouse effect, sunlight penetrates through the atmosphere (in the visible) but the thermal energy to be reradiated by the planetary surface in the infrared is trapped because of the infrared opacity of the planetary atmosphere resulting from abundant $CO_2$ and $H_2O$. Thermal blanketing is more severe, because solar radiation incident on the top of the atmosphere is completely scattered by the fine aerosols and impact ejecta and all the thermal energy is absorbed by the greenhouse gases, $H_2O$ and $CO_2$. Impact cratering calculations (Ahrens et al 1989, O'Keefe & Ahrens 1977a) demonstrate that for large impactors, 60 to 90% of the energy of the impact is delivered as internal energy of the near surface material. The major effect of the proto-atmosphere then is to provide an insulating blanket to the flux of heat due to impacts on the surface of the growing planet. These processes are described by the equation

$$(1 + 1/2\theta)\frac{Gm_p}{R_p}\dot{m}dt = 4\pi R^2(F_{atm} - F_i)dt + C_p\dot{m}_p(T_s - T_p)dt + C_p m_s \dot{T}_s dt, \tag{10}$$

where the left-hand side is the rate of kinetic energy supplied to the surface provided by the impacting planetesimals. The first term on the right is the

balance of heat flux of the atmosphere, where $F_{atm}$ is the energy flux escaping from the surface to interplanetary space and $F_i$ is the energy flux from the interior to the surface layer. The second and third terms are the heat sinks to the planet as a result of heating a larger planetary material of mass $m_s$ from planetesimal temperature $T_p$ to the higher surface temperature $T_s$. For a graybody radiative equilibrium atmosphere

$$F_{atm} = 2(\sigma T_s^4 - S_0/4)/[(3kp_0/2g)+2], \quad (11)$$

where $\sigma$ is the Stefan-Boltzmann constant, $S_0$ is the solar flux, $k$ is the absorption coefficient in the atmosphere, and $p_0$ is the surface pressure. Thermal blanketing as described by Equations 10 and 11, with the reasonable values of the constants chosen by Abe & Matsui (1985, 1986), quickly leads to temperatures above the solidus of crustal (basaltic) rocks (Figure 6*a*). Moreover, as more planetesimals impact the planet, the additional water provided begins to dissolve in what is the start of a magma ocean. Abe & Matsui showed that the surface temperature should be buffered by the solidus of hydrous basalt, $\sim$1500 K, and the mass of $H_2O$ in the atmosphere is nearly constant at $10^{24}$ g (essentially the present surface water budget) (Figure 6*b*). They showed that the mass of $H_2O$ in the atmosphere remains nearly constant (due to a negative feedback effect). This effect can be demonstrated for a small surface temperature increase. This causes an increase in the fraction of molten basalt. That in turn induces additional water to dissolve in the molten silicate. Loss of water from the atmosphere then decreases the effectiveness of atmospheric blanketing and the result is that the small increase in temperature is nullified by the system's negative feedback.

The effectiveness of thermal blanketing of impact energy by the massive proto-atmosphere, as well as the feedback effect of water solubility in molten silicates, has been independently verified in a study by Zahnle et al (1988).

The termination of the coaccretion of an atmosphere and planet, which was modeled to occur on Earth, Venus, and Mars, can occur via three different mechanisms.

1. Abe & Matsui (1988) suggested that as the accretion rate decreased, the impact energy flux at the base of the atmosphere decreased and gradually solar heating dominated over impact heating. The surface temperature then declined below the melting point of hydrous basalt. With decreasing temperature, the water condensed and formed terrestrial oceans. Oceans may have formed on Venus (Matsui & Abe 1986b)—however, the larger solar ultraviolet flux gives rise to an enhanced photodisassociation to hydrogen and oxygen in the upper

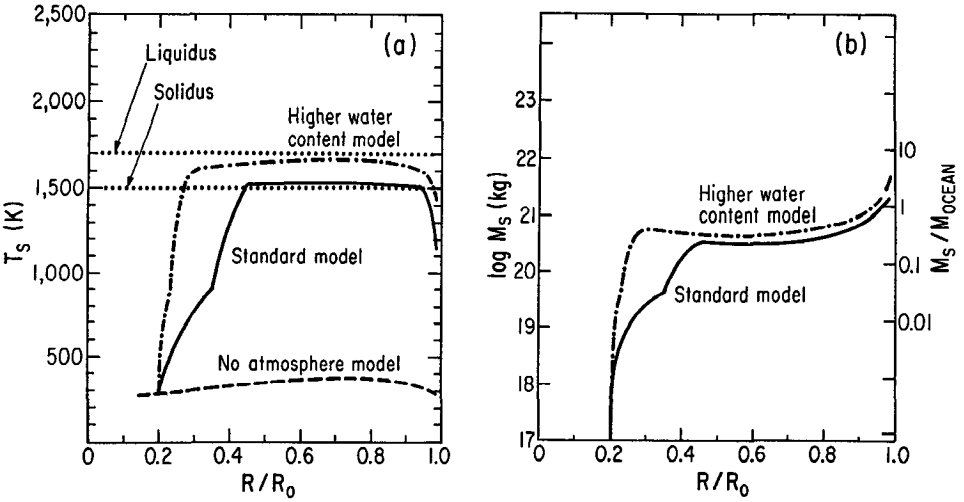


*Figure 6* (*a*) The evolution of surface temperature during accretion of a model Earth from planetesimals containing 0.1% $H_2O$. The radius $R$ is normalized by the final value, $R_0$. The dashed curve gives the calculated surface temperature without an impact-generated atmosphere (accretion period is $5 \times 10^7$ yr). The model surface temperature is affected by an atmosphere (which begins to greatly increase its mass once the impact velocity exceeds a critical value). The rapid rise in the surface temperature of the "standard model" which occurs after the Earth grows to $\sim 0.3R_0$, is due to an increase in the total mass of the atmosphere because of the initiation of the complete dehydration reaction of the surface layer. Once the surface temperature reaches the melting temperature, it remains nearly constant. [Figure after Matsui & Abe (1986a).] (*b*) The total mass of the impact-generated $H_2O$ atmosphere is plotted against the normalized radius for the standard planetesimal models. Note that the total atmospheric mass, $M_s$, remains nearly constant after the Earth grows to $0.4R_0$ and is very close to the present mass of the Earth's oceans ($1.4 \times 10^{21}$ kg). [Figure after Matsui & Abe (1986a).]

atmosphere and subsequent Jeans escape of a large fraction of the planet's hydrogen inventory gives rise to the presently observed enhancement of the D/H ratio of Venus relative to the Earth of $\sim 10^2$.

2. Atmospheric loss occurs via multiple impact erosion. This is discussed in the next section.
3. Sudden partial or complete atmospheric loss occurs as a result of a large body impact. This is discussed in Section 8.

## 7. ATMOSPHERIC EROSION BY IMPACT CRATERING

In addition to bringing volatiles to accreting atmospheres, the infall of planetesimals can erode planets and their oceans and atmospheres. For

atmosphere-free solid and molten silicate planets, because the mechanical impedance of the impacting planetesimals is, in general, similar to that of a planet, the amount of ejecta which can escape from a planet with a given surface escape velocity depends only on impact velocity (and hence energy per unit mass) (O'Keefe & Ahrens 1977b), whereas the net gain or loss of a planetary atmosphere depends on total impact energy. O'Keefe & Ahrens (1982) calculated the energy partitioning into an atmosphere overlying a planet. They found that upon impact of a planet with projectiles of radii less than the atmospheric scale height, where the ejecta was primarily solid or molten, the amount of energy imparted to the atmosphere by direct passage through the atmosphere was only a few percent. Moreover, very little of the atmosphere achieved upward velocities in excess of the escape velocity. Walker (1986) showed that a very small portion of the atmosphere, shocked by the meteoroid, achieved sufficient enthalpy density to expand to greater than escape velocity. Using a numerical explosion model, Jones & Kodis (1982) showed that for the Earth, atmospheric explosion energies $>5\times10^{26}$ ergs induced significant atmospheric blow-off.

Subsequently, Ahrens & O'Keefe (1987) and Ahrens et al (1989) employed a model in which they assumed all the energy of the impactor is delivered to the planetary surface and applied a theory [developed by Zel'dovich & Raizer (1966, Chapter 12) and Bach et al (1975)] for the shock acceleration of the atmosphere by an explosion (Figure 7). In this model, the time for atmospheric escape is related to atmospheric density near the Earth's surface, $\rho_{00}$, explosion energy, $E$, and atmospheric scale height, $H$, by

$$t = C_1(\rho_{00}H^5/E)^{1/2}, \tag{12}$$

where the constant, $C_1$, is approximately equal to 25. Moreover, the initial atmospheric shock velocity for atmospheric escape is

$$D = \alpha H/t, \tag{13}$$

where $\alpha \cong 6$. Assuming the Earth impactor has a velocity $v_e = 11$ km/sec and a strong shock condition exists such that $D \cong 11$ km/sec, Equation 13 yields $t = 4.4$ sec and the minimum impact energy calculated from Equation 12 is $1.9\times10^{27}$ ergs. A projectile carrying this energy, if composed of silicate, will have a radius of $\sim0.5$ km. The energy, $1.9\times10^{27}$ ergs, is somewhat greater (by a factor of 20) than that from the numerical calculations of Jones & Kodis (1982).

For more energetic impacts (larger impactors), Melosh & Vickery (1989) and Vickery & Melosh (1990) developed a simple atmospheric cratering model applicable, for example, on the Earth in the $4.5\times10^{27}$ to $9.9\times10^{30}$

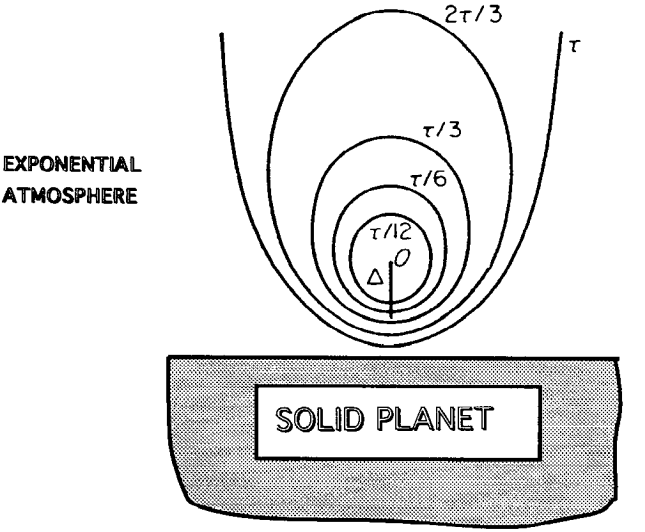


*Figure 7* Shock front at successive instants of time for a strong explosion at high altitude. Sections shown are formed by passing a vertical plane through the origin of the explosion. The density of the atmosphere changes by a factor of $e$ over the atmospheric scale height, $\Delta$. Note that $\tau = (\rho_c \Delta^5/E)^{1/2}$, where $\rho_c$ is the density at the altitude of the explosion and $E$ is the energy. (After Zel'dovich & Raizer 1966.)

erg energy range (Figure 8). For 20 km/sec, 2.7 g/cm$^3$ impactors, these energies correspond to impactor radii of 0.6 to 7.6 km. They pointed out that for high-velocity planetary impacts, which penetrate the atmosphere, the projectile and a proportional mass of target become vaporized. For simplicity they assumed that the mass vaporized is equal to twice the mass of the impactor. This assumption is consistent with detailed computer simulation of impact on planetary surfaces (O'Keefe & Ahrens 1977a). The resulting gas plume then expands at a speed greater than the planetary escape velocity and carries with it the overlying planetary atmosphere. A conservative model of the plume expansion gives the mean (mass-averaged) velocity of expansion as

$$v_{exp} = [2(e - h_{vap})]^{1/2}, \tag{14}$$

where $e$ is the internal energy per unit mass of the impactor and $h_{vap}$ is the total enthalpy per unit mass, starting at the ambient temperature required to vaporize the projectile or target material. For silicate and ice, $h_{vap}$ is $13 \times 10^{13}$ and $3 \times 10^{13}$ ergs/g, respectively. The energy per unit mass imparted by the impact-induced shock wave for like materials is $e \approx v^2/8$,

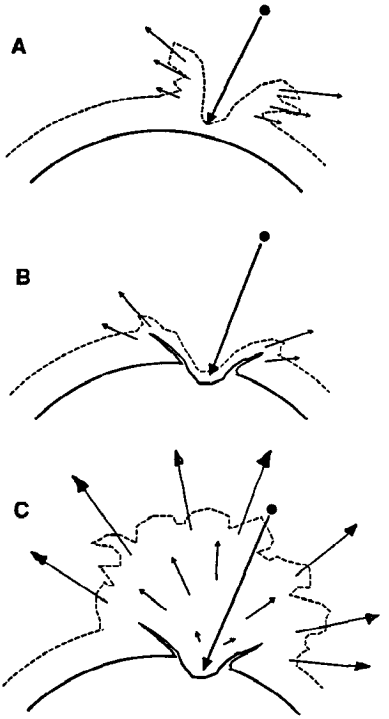


*Figure 8* Cartoons of atmospheric impact indicating how projectile momentum can be transferred to a planetary atmosphere. (*A*) The projectile enters the atmosphere, heating, compressing, and accelerating the atmospheric gases ahead of it. (*B*) Solid ejecta from a growing crater pass through the atmosphere, transferring some or all of their momentum to the atmosphere by drag. Only a small quantity of atmosphere is ejected via the mechanisms of *A* and *B*. (*C*) The impact-generated vapor plume expands upward and outward. (After Vickery & Melosh 1990.)

where we assume the shock particle velocity $u$ is $v/2$. It is easy to show that the minimum impact velocity required for the vapor plume to exceed the escape velocity is

$$v_m = \sqrt{8[(v_e^2/2)+h_{vap}]}. \quad (15)$$

Atmospheric erosion occurs if the impact-induced momentum of this shock-induced gas when combined with the mass of the overlying atmosphere has sufficient velocity to escape the planet. By assuming a self-similar velocity profile in the total expanding gas cloud proposed by Zel'dovich & Raizer (1966, p. 104) of the form

$$\rho(r) = A(1-r^2/R^2)^\alpha/R^3, \quad (16)$$

where $R$ is the radius of the front of the gas cloud and $r$ is the radius to a point within the gas cloud, $A$ and $\alpha$ are determined by assuming conservation of mass and energy above the impact site. Vickery & Melosh (1990) used a value of $\gamma = 9/7$ to infer values of $\alpha = 11$ and $A = 15.4M_t$,

where $\gamma$ is the gas cloud's polytropic exponent, and $M_t$ is the total mass of the vapor cloud. When the projectile velocity exceeds the minimum impact velocity for atmospheric escape (Equation 15), escape occurs in atmosphere directly above the impact site. As the impact energy is increased, a cone with increasing angle $\theta$ is ejected (Figure 9). As impacts become more energetic, the maximum energy in the Vickery-Melosh model corresponds to ejection of an air mass above the tangent plane (Figure 9) of $3 \times 10^{18}$ g (for the case of the Earth) or $6 \times 10^{-4}$ of the total atmospheric budget. Vickery & Melosh showed that, for the case of the above approximations, when the mass of the projectile exceeds the mass of the atmosphere above the horizontal tangent, $m_c$, all of the atmosphere above a tangent plane to Earth is ejected. Thus when

$$m \geq m_c \equiv Hm_a/2R_p \tag{17}$$

Equation 17 indicates that for smaller $m_a$, the mass of the atmosphere gives rise to a smaller mass $m_c$, which can erode an atmosphere. Table 1 gives $m_c$ values for the terrestrial planets. Since smaller projectiles are more numerous and thinner atmospheres erode rapidly, Equation 17 indicates that once an atmosphere starts eroding, erosion is accelerated until the planet is stripped. Figure 10 shows the maximum atmospheric mass that can be expelled by a spectrum of impactors for three different planets for

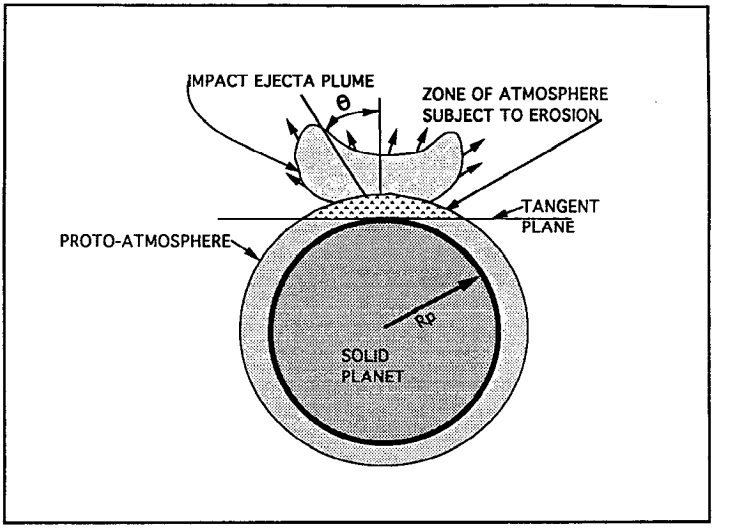


*Figure 9* The impact-generated gas is assumed to interact only with the atmosphere lying above the plane tangent to the Earth at the center of impact. (After Vickery & Melosh 1990.)

**Table 1** Characteristics of impact erosion models

| | Vickery-Melosh model | |
|---|---|---|
| Planet | Tangent mass (g) | Tangent mass, impact energy (ergs) |
| Earth | $2.6 \times 10^{18}$ | $9.9 \times 10^{30}$ |
| Venus | $5.9 \times 10^{20}$ | $1.6 \times 10^{33}$ |
| Mars | $4.4 \times 10^{16}$ | $4.5 \times 10^{28}$ |

| | Total blow-off model | | | |
|---|---|---|---|---|
| | Free-surface velocity for atmospheric escape (km/sec) | | Impact energy for total blow-off (ergs) | |
| Planet | $\gamma = 1.1$ | $\gamma = 1.3$ | $\gamma = 1.1$ | $\gamma = 1.3$ |
| Earth | 1.60 | 2.75 | $6.20 \times 10^{37}$ | $1.84 \times 10^{38}$ |
| Venus | 1.00 | 2.45 | $2.10 \times 10^{36}$ | $1.20 \times 10^{37}$ |
| Mars | 1.03 | 1.20 | $2.90 \times 10^{34}$ | $5.70 \times 10^{35}$ |

a given accretion (veneer) mass being added to the planet. Melosh & Vickery (1989) demonstrated how Mars' atmosphere could have been eroded from an initial surface pressure of 0.7 bars to the present $7 \times 10^{-3}$ bars in the first 1.4 Gyr of solar system history.

In conclusion, note that in the case of the Earth, impact erosion is important only for impacts more energetic than $\sim 10^{27}$ ergs. Thus the Abe-Matsui scenario, which only deals with atmospheric accretion, is relevant if the projectiles impacting the Earth's surface are much smaller in radius than the atmospheric scale height. For projectiles with radii in the km range, the research summarized in this section indicates that impact erosion needs to be taken into account in accretion models of the terrestrial planets.

## 8. ATMOSPHERIC BLOW-OFF BY GIANT IMPACTS

As discussed in Section 3, as the planets accreted according to the Safronov-Wetherill-Kaula scenario, the planetesimal impactors also grew in size and it appears likely that some planetesimals grew to radii in the 2000 to 3000 km range—comparable to the size of the smaller planets (e.g. Mercury and Mars). These considerations have motivated the numerical modeling of large body impacts by Benz et al and Kipp & Melosh cited in Section 5.

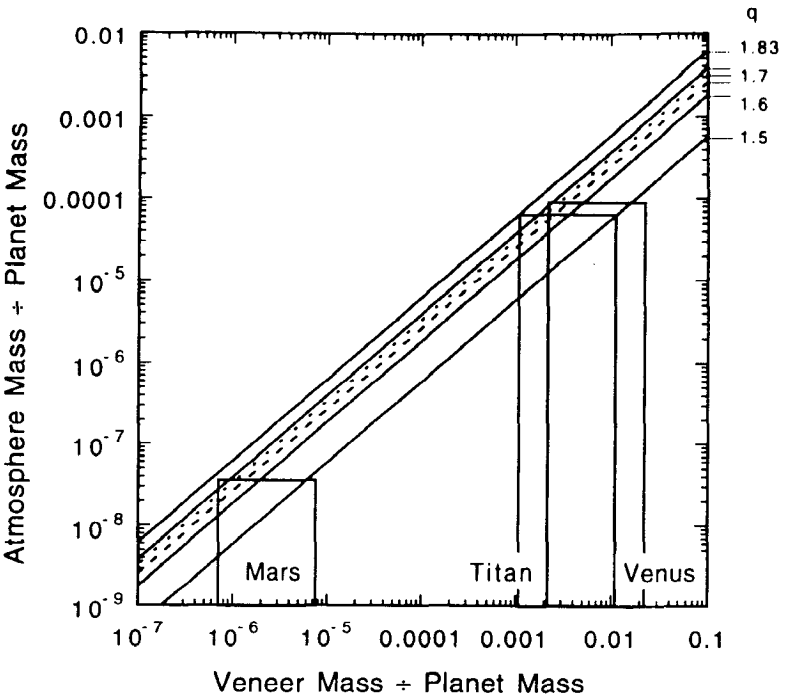


*Figure 10* The normalized maximum atmospheric mass that can be expelled by an impacting veneer of normalized mass for three values of $q$, the power law exponent describing the (differential) mass spectrum of impactors. Mars (*dots*) and Venus (*dashes*) are quantitatively similar (both shown for $q = 1.7$). Rectangles indicate veneer masses (width corresponds to plausible $q$ values) needed to remove present atmospheres of Titan, Mars, and Venus. (After Zahnle et al 1992.)

Previously, the effects of large body impact on the Earth's atmosphere have only been briefly described by Ahrens (1990). To calculate the energy, and hence, approximate planetesimal size, such that upon impact the entire planetary atmosphere is blown off, I employ a different approach than previous efforts and consider a shock wave that is entirely propagated within a terrestrial planet as sketched in Figure 11.

For a large impact on a terrestrial planet, where the impactor dimensions are greater than the atmospheric scale height (Table 2), the direct shock wave strips the atmosphere in the vicinity of the impactor (Figure 9). The air shock is also refracted around the entire planet. However, most of the projectile energy will be delivered to the solid planet (O'Keefe et al 1982). The effect on the overlying atmosphere of a great impact on the solid planet is considered below.

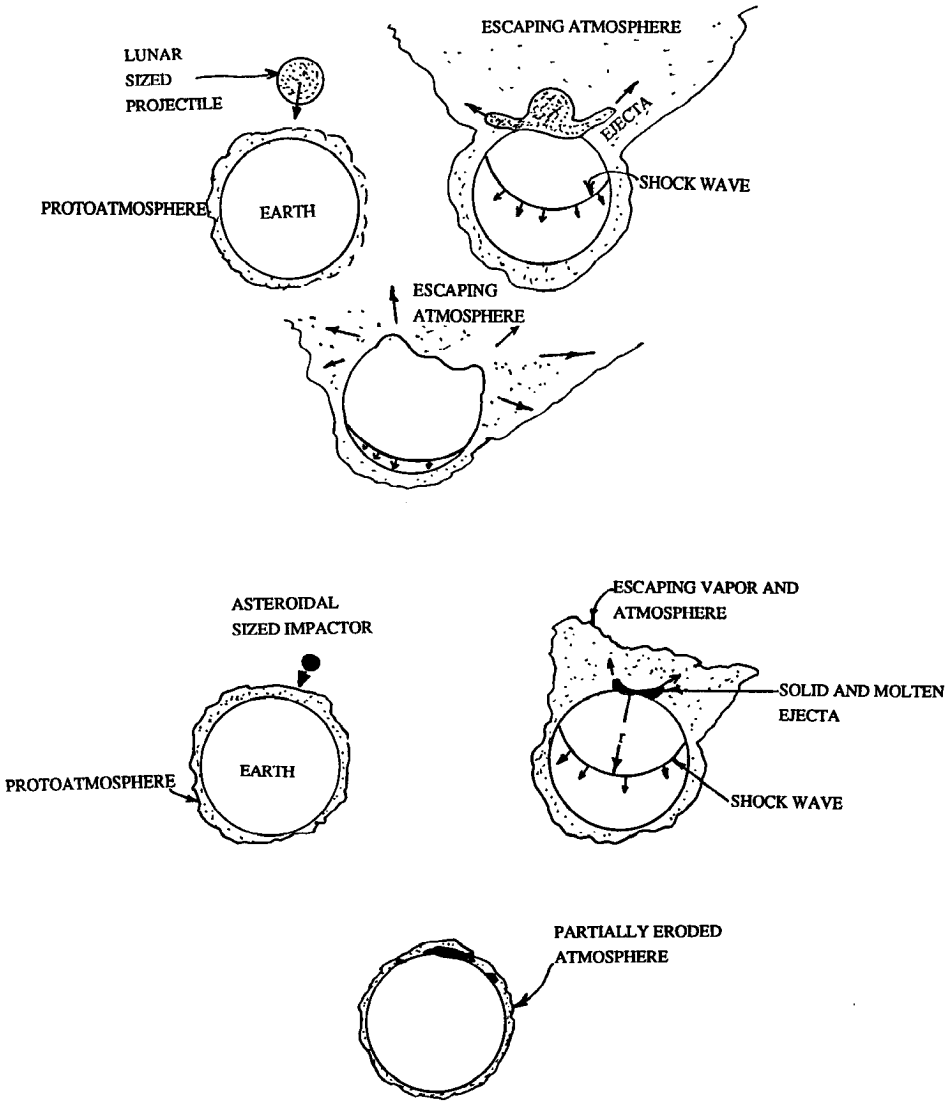


*Figure 11* (*Top*) Sketch of lunar-sized planetesimal impacting the Earth. The proto-atmosphere is blown away by the shock wave-induced motion of the solid or molten planet. (*Bottom*) Impact of asteroidal-sized impactor and resultant partial eroded atmosphere.

**Table 2** Terrestrial planet and atmosphere properties

| | Solid planet | | | |
|---|---|---|---|---|
| Planet | Radius (km) | Core radius (km) | Surface gravity ($cm/sec^2$) | Surface escape velocity (km/sec) |
| Earth | 6352 | 2769 | 981 | 11.18 |
| Venus | 6052 | 2827 | 887 | 10.37 |
| Mars | 3396 | 1146 | 372 | 5.03 |

| | Atmosphere | | | | |
|---|---|---|---|---|---|
| Planet | Molecular weight (daltons) | Surface pressure (bars) | Scale height (km) | Surface temperature (K) | Surface density ($g/cm^3$) |
| Earth | 29 | 1.01 | 8 | 288 | $1.29 \times 10^{-3}$ |
| Venus | 44 | 92 | 15 | 735 | $6.49 \times 10^{-2}$ |
| Mars | 44 | 0.007 | 11 | 215 | $1.20 \times 10^{-5}$ |

The key calculation is to relate the particle velocity of the solid planet-atmosphere interface, $u_{fs}$, antipodal of a major impact to the atmospheric free-surface velocity, $v_e$. The velocity, $v_e$, is achieved as a result of the atmosphere being shocked first by the solid planet moving at velocity $v_{fs}$, and then becoming further accelerated to velocity, $v_e$, as a result of the upward propagating shock wave reflecting (isentropically) at the effective top of the atmosphere (Figure 12). This reflection provides an additional velocity increment, $u_r$. Gas speeds greater than the escape velocity are thus achieved. This is a conservative calculation since I use the density and pressure of the atmosphere at its base. Moreover, the atmosphere covering the planet closer to the impact than the antipode is expected to achieve yet higher velocity because it is shocked by the decaying air wave, and also shocked to higher pressures by the solid planet. Note that, in general, as a shock wave is propagated upward in an exponential atmosphere, because the density encountered by the traveling shock is decreasing, the shock velocity and particle velocity increase with altitude as discussed in Section 6 and by Zel'dovich & Raizer (1966). Thus, one can safely neglect shock attenuation in the atmosphere, and assume the particle velocity at the solid planet-atmosphere interface (the independent variable) and calculate the shock pressure induced in the gas by the outward surface of the Earth. The solid Earth therefore acts like a piston with velocity, $u_{fs}$, pushing on the atmosphere.

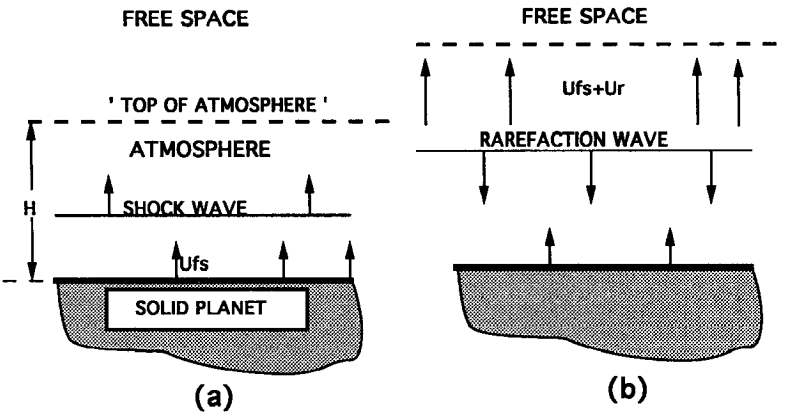


*Figure 12* Sketch of shock- and rarefaction wave-induced motion of atmosphere being driven by planetary free-surface velocity, $u_{fs}$. Atmosphere geometry is approximated by a layer of scale height, $H$. (*a*) Shock wave driven particle velocity, $u_{fs}$. (*b*) Increase of gas velocity to $u_{fs}+u_r$ upon "reflection" of shock at the "top of atmosphere."

The pressure behind the shock wave, $p_1$, for different outward rock velocities, $u_{fs}$, can be determined by solving for $p_1$ in the following set of equations (e.g. Equations 1.78 and 1.79 of Zel'dovich & Raizer 1966):

$$|u_{fs}| = u_0 - u_1, \tag{18}$$

where

$$u_0 = \{V_0[(\gamma-1)p_0+(\gamma+1)p_1]/2\}^{1/2} \tag{19}$$

is the particle velocity of the unshocked gas with respect to the shock wave in the atmosphere and

$$u_1 = \left\{\frac{V_0[(\gamma+1)p_0+(\gamma-1)p_1]^2}{2[(\gamma-1)p_0+(\gamma+1)p_1]}\right\}^{1/2}, \tag{20}$$

where $u_1$ is the particle velocity of the shocked atmosphere relative to the shock front. Surface values of $p_0$ and $V_0 = 1/\rho_{00}$ for the planetary atmospheres used to calculate $p_1$ are given in Table 2. As shown in Figure 7, the upward propagation of the shock wave in a decreasing atmosphere gives rise to a great increase in both shock and particle velocity which we approximate by imagining that this shock "reflects" at the "top of the atmosphere" at a scale height, $H$. This is sketched in Figure 12*b*. This approximation should be valid if the duration of the impact induced particle velocity, $u_{fs}$ ($\sim 10^2$ sec, see Figure 14), is long compared to the

travel time ($\sim$20 sec) of a sound wave in the atmosphere up to a scale height.

Upon reflection of the shock wave at the top of the atmosphere, isentropic release from $p_1$ to zero pressure gives rise to an additional large increase in particle velocity which is described by the Riemann integral:

$$u_r = \int_0^{p_1} (-dV/dp)^{1/2}\, dp. \tag{21}$$

Upon substituting for an ideal polytropic gas, with a polytropic exponent, $\gamma$, Equation 21 yields

$$u_r = (p_0^{1/\gamma} V_0/\gamma)^{1/2} p_1^{1/2 - 1/(2\gamma)}/[1/2 - 1/(2\gamma)]. \tag{22}$$

The shock-induced outward atmospheric velocity, $u_e$, is given by

$$u_e = |u_{fs}| + u_r. \tag{23}$$

We assume that when

$$|u_e \geq v_e| \tag{24}$$

atmospheric blow-off occurs. When $u_e = v_e$, the corresponding value of $u_{fs}$ is denoted by $u_{fse}$. The outward rock velocity versus outward atmospheric velocity for the Earth, Venus, and Mars, is shown in Figure 13 for values of the polytropic exponent in the range from 1.1 to 1.3. This range encompasses the effective likely range of $\gamma$ which is expected to decrease from 1.3 to 1.1 with increasing gas ionization. Equation 24 is satisfied for $\gamma = 1.1$ to 1.3 for outward rock velocities of 1.60 to 2.25 km/sec for Earth, 1.00 to 2.45 km/sec, for Venus, and 0.27 to 1.2 km/sec for Mars. What impact energies will produce these outward rock velocities for the terrestrial planets?

Fortunately, the strength of the shock-wave induced compressional wave that results upon propagation completely through planets with varying iron core sizes overlain by silicate mantles has been recently calculated for objects that have core to planetary radius ratios of 0.333 and 0.466 (Watts et al 1991). In these calculations, the energy of the surface source was $E_w = 3.1 \times 10^{34}$ ergs. Notably, the calculation of Watts et al (1991), when scaled as discussed below, agrees closely with those of Hughes et al (1977) upon which earlier estimates of the energy required to blow-off the Earth's atmosphere were based (Ahrens 1990).

I scaled the results, which are given as peak compressional wave stresses experienced by material directly beneath the antipode of the impact point for a core to planetary radius ratio of 0.333 and a planet radius $R_w = 1500$ km, to that for Mars, which has a core to radius ratio of $\sim$0.34 and a

planetary radius of $R_p = 3396$ km (Table 2). Similarly, I used the Watts et al result for a core to planetary radius ratio of 0.47 to provide estimates of the peak stress beneath the antipode for an impact on the Earth and Venus for which the actual core to planetary radius ratios are 0.44 and 0.47, respectively. Since planetary gravity was not included in the calculations, we employ cube scaling (Melosh 1989, p. 112) to adjust the results for planetary size.

The energy of the equivalent surface source, $E_p$, assumed for an impact on the actual planet of interest is

$$E_p = E_w(R_p/R_w)^3. \tag{25}$$

To relate the peak pressure experienced by the cell beneath the antipodes for the 0.33 and 0.47 core to planetary radius ratios, peak shock pressures of $P_1 = 2.03$ and $P_1 = 2.10$ GPa were used. To convert these values to shock particle velocity, $u_1$, I assumed a surface density of $\rho_0 = 2.72$ g/cm$^3$ and a shock velocity $U_s = 5$ km/sec in the momentum equation:

$$u_1 = P_1/(\rho_0 U_s) \tag{26}$$

and then made the common approximation that the outward rock (free-surface) velocity $u_{fsw}$ corresponding to the Watts et al calculation is

$$u_{fsw} = 2u_1. \tag{27}$$

The energy $E_{fs}$, required of an impactor to obtain the upper and lower bounds of $u_{fs}$ necessary to launch the atmosphere to escape velocity in the calculations of Figure 13, can then be calculated from

$$E_{fs} = E_p(u_{fs}/u_{fsw})^2. \tag{28}$$

Thus, for complete atmospheric blow-off, values for $E_{fs}$ of $6.2 \times 10^{37}$ to $1.8 \times 10^{38}$ ergs are inferred for the compressional wave induced motion for the Earth. This compares to $\sim 10^{37}$ ergs previously calculated for the compressional wave by Ahrens (1990). For Venus, $E_{fs}$ varies from $2.1 \times 10^{36}$ to $1.2 \times 10^{37}$ ergs, whereas for Mars values of $2.9 \times 10^{34}$ to $5.7 \times 10^{35}$ ergs are needed for complete blow-off (Table 1).

The above impact energies may be somewhat of an overestimate as the later arriving antipodal surface (Rayleigh) wave is expected to have a greater vertical amplitude, and hence, higher free-surface velocity.

Although calculation of antipodal compressional wave amplitude via finite difference methods, such as employed by Hughes et al and Watts et al are straightforward, obtaining surface wave forms requires more computational effort. Recently, H. Kanamori (private communication, 1992) has calculated the antipodal surface wave displacement for the Earth for a point force step pulse of $10^{16}$ dynes (Figure 14) using the method of

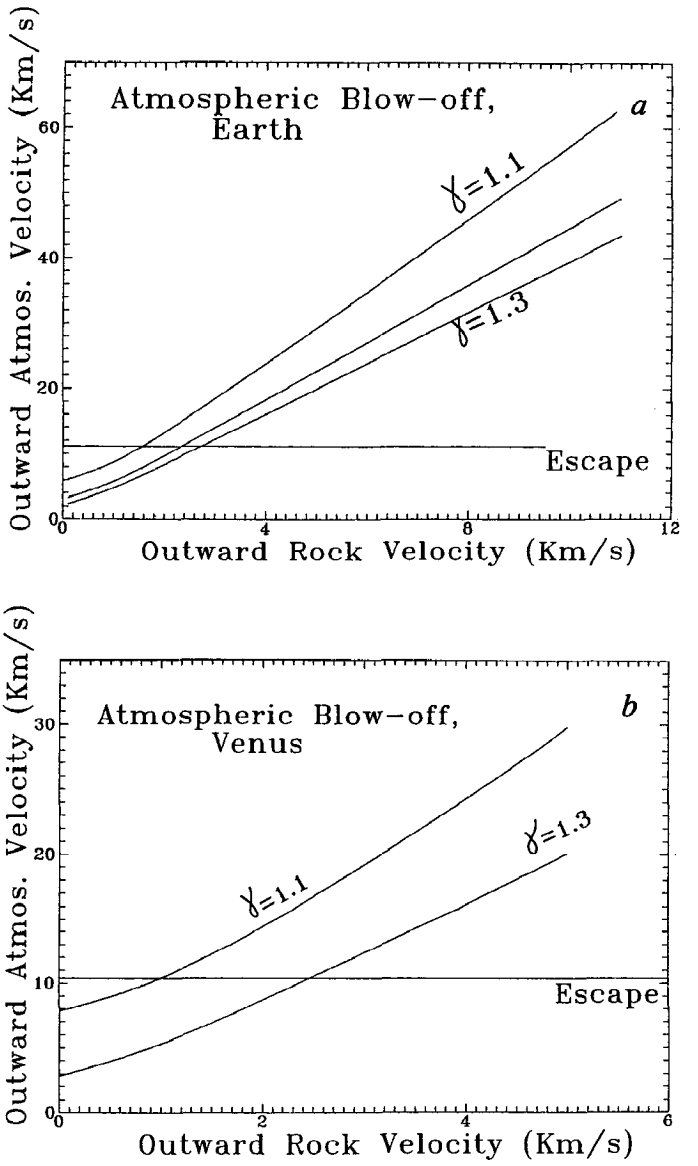


*Figure 13* Relationship of outward free-surface velocity ($u_{fs}$) to outward atmospheric velocity ($v_e$) for a polytropic atmosphere with various values of $\gamma$. (*a*) Earth, (*b*) Venus, (*c*) Mars.

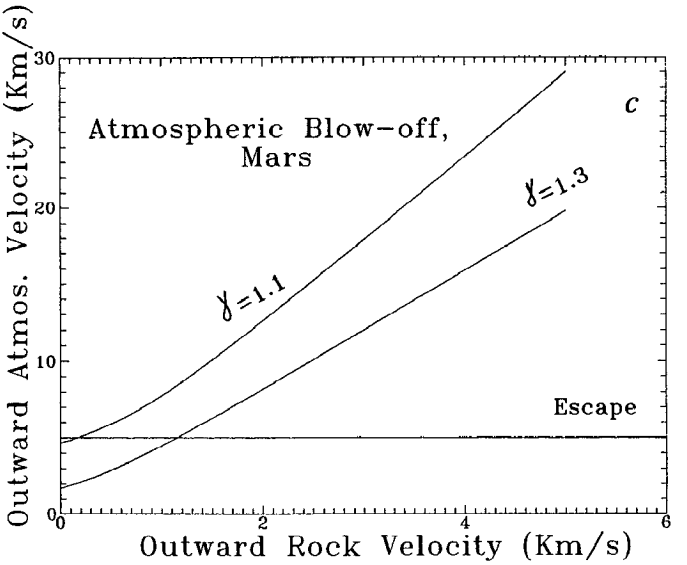


*Figure 13* (*continued*).

Båth (1966). Because the elastic displacement at the source is singular, it is convenient to estimate the energy in the surface wave as it passes over the equator (relative to the source region) from the equation (Kanamori & Hauksson 1992):

$$E \cong 2\pi(2\pi R_p)\bar{h}U \int_0^\infty \dot{x}(t)dt, \tag{29}$$

where $R_p$ is the Earth's radius, $\bar{h} = 3 \times 10^7$ cm is approximately 1/3 the wavelength of the fundamental Rayleigh wave Airy phase, $U = 3.6 \times 10^5$ cm/sec is the group velocity, and $\rho = 2.7$ g/cm$^3$. We assume that the peak to peak displacement of Figure 14*b* occurs over a period of $\sim$200 sec. Moreover, the integral is approximated by a 400 sec time interval. Thus Equation 29 yields an energy of $E = 2.6 \times 10^{11}$ ergs. Application of the same scaling as used in Equation 28, for the Earth, yields a seismic energy of 8 to $16 \times 10^{34}$ ergs for $\gamma = 1.3$ and 1.1, respectively. Although this is a factor of $10^3$ to $10^4$ lower than is given for the energy inferred from body wave amplitudes (after Equation 28), the inefficiency of inducing a seismic surface wave from a surface hypervelocity impact needs to be taken into account. This factor is poorly known. Schultz & Gault (1975) estimate only $10^{-3}$ to $10^{-4}$ of the impact energy is carried from the impact region away as seismic energy. Their estimate may be too low for a giant impact.

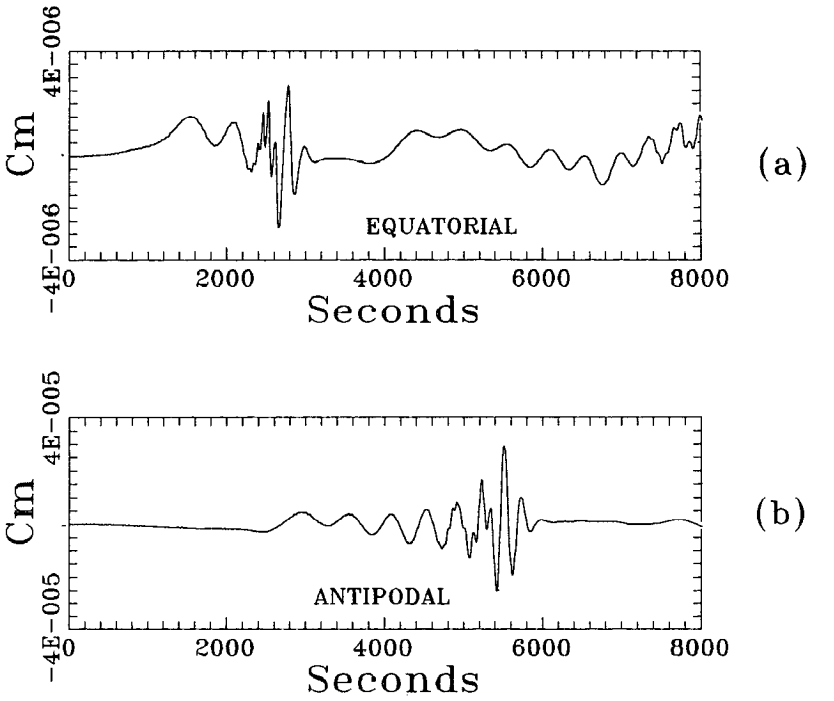


*Figure 14* Theoretical free-surface elastic displacement of the Earth versus time upon sudden application of a surface (point) source of $10^{16}$ dynes. (*a*) Displacement history at 90° (equatorial) from source. (*b*) At 180° (antipodal) from the source. [After H. Kanamori (private communication, 1992).]

More research is obviously needed. Nevertheless, with our present knowledge of cratering mechanics, it appears difficult to estimate the expected difference between body and surface wave induced atmospheric blow-off, and the energy estimates given on the basis of body waves should be tentatively accepted as the best order-of-magnitude estimate. Clearly, estimating antipodal surface wave amplitudes for large impacts on the other terrestrial planets, is even more uncertain and is not attempted here.

Finally, it is useful to estimate the energy and mass fraction of the planetary atmosphere blown off in going from the Melosh-Vickery model of tangential blow-off (Table 1) to the condition of complete blow-off. For energies less than those required to eject the entire atmosphere, I assume a simple power law for the decrease of particle velocity with radius, $r$, from the impact point (Figure 11*b*) and assume that as the decaying stress wave interacts with the free-surface of a spherical planet, atmospheric blow-off

occurs if the particle velocity is greater or equal to 0.5 $u_{fse}$—which is the value of $u_{fs}$ required to blow off the atmosphere for the antipodal case. Thus, the amount of atmosphere blown off is related to the area of a sphere subtended by an arc of radius $r$ at the point where the particle velocity has decayed to 0.5 $u_{fse}$ (Figure 11*b*).

To determine an empirical relation for the attenuation of particle velocity, I assume the form (Melosh 1989, p. 62):

$$u = u_0/r^n. \tag{30}$$

I first calculate the radius of a hemisphere, $r_1$, enclosing a unit mass

$$r_1 = [3/(2\pi\rho_0)]^{1/3}. \tag{31}$$

Using the values of $E_{fs\,min}$ and $E_{fs\,max}$ calculated from Equation 28 to designate the minimum and maximum energies obtained from Figure 13 for $\gamma = 1.1$ and $\gamma = 1.3$, respectively, the shock particle velocity associated with each energy is given by

$$u_{1\,min} = (E_{fs\,min})^{1/2} \tag{32a}$$

$$u_{1\,max} = (E_{fs\,max})^{1/2}. \tag{32b}$$

Denoting $|u_{fs}|$ calculated from Equation 18 using $\gamma = 1.1$ and $\gamma = 1.3$ as $u_{fs\,min}$ and $u_{fs\,max}$ I can obtain from Equations 27 and 30, expressions for the particle velocity decay parameters, $n_1$ and $n_2$:

$$n_1 = \log(2u_{1\,min}/u_{fs\,min})/\log(2R_p/r_1) \tag{33a}$$

$$n_2 = \log(2u_{1\,max}/u_{fs\,max})/\log(2R_p/r_1). \tag{33b}$$

For a stress wave particle velocity which decays to a value of $u_{fsw}/2$ at a radius $r_e$ from the impact point, the mass of atmosphere blown off is

$$m_e = (p_0/g)A, \tag{34}$$

where the term in parentheses is the atmospheric mass per unit area and $A$ is the area of a sphere subtended by an arc of length $r$ (Figure 11*b*).

From geometrical arguments it can be shown that the area of the planet subtended by an arc of length $r$ is

$$A = \pi r^2. \tag{35}$$

The energies (minimum and maximum) associated with the radius $r_e$, for $\gamma = 1.3$ and $\gamma = 1.1$ values are:

$$E_{min} = [u_{fs\,min}(r_e/r_1)^{n_1}/2]^2 \tag{36a}$$

$$E_{max} = [u_{fs\,max}(r_e/r_1)^{n_1}/2]^2. \tag{36b}$$

The normalized mass of the atmosphere blown off, $m_e/m_a$, versus both $E_{min}$ and $E_{max}$ are shown in Figure 15.

Table 1 shows that the energy for atmospheric loss above a tangent plane is a small fraction ($\sim 10^{-8}$ to $10^{-4}$) of the energy required to drive off the entire atmosphere. For the Earth, this total loss energy is $\sim 10^{38}$ ergs and would be achieved via an impact of a lunar-sized object at 20 km/sec. In the case of Venus, the impact of a smaller $\sim 800$ km radius object, at $\sim 20$ km/sec, will drive off the atmosphere. For Mars, the impact of a 160 km radius object at 20 km/sec will drive off the atmosphere. It may be, as suggested by Cameron (1983), that the terrestrial planets all suffered several giant impacts and their present atmospheres may reflect accretion and outgassing since the last great impact event.



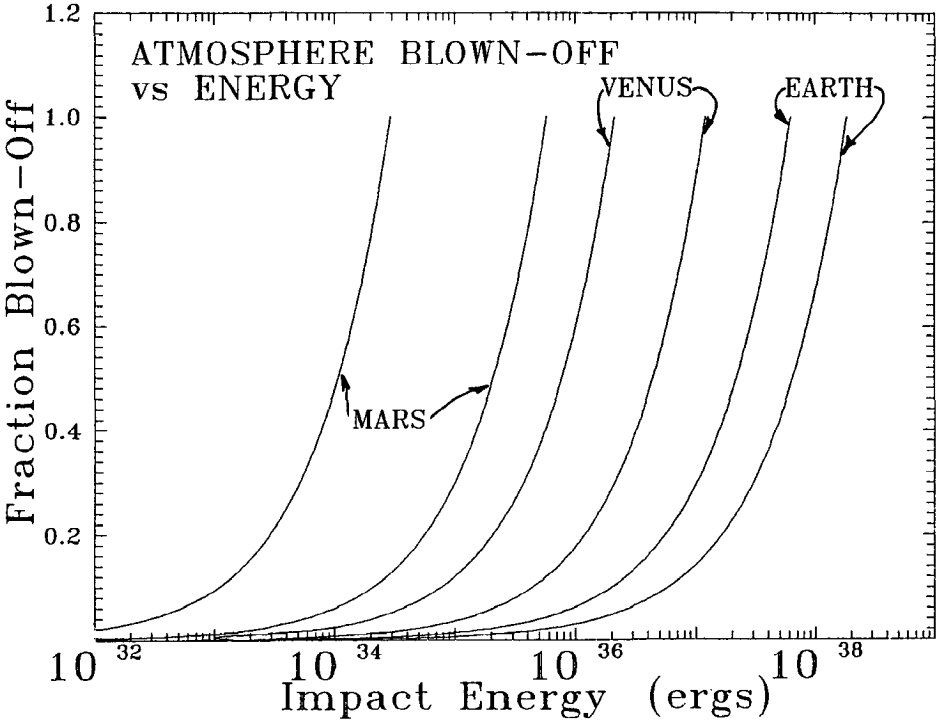


*Figure 15* Calculated fraction of atmosphere blown off versus impactor energy for Earth, Venus, and Mars. Lower and higher energy curves for each planet correspond to assumed polytropic exponent of ideal gas of $\gamma = 1.1$ and 1.3, respectively.

ACKNOWLEDGMENTS

I appreciate receiving helpful comments on this paper from G. W. Wetherill, A. Vickery, A. W. Harris, and L. R. Rowan, as well as private communications from G. Chen and J. Melosh. Special thanks go to H. Kanamori who computed the results shown in Figure 14. Many of the ideas developed in this review have come from collaborations with J. D. O'Keefe, M. A. Lange, and J. A. Tyburczy. This research is supported by NASA and is Contribution #5198, Division of Geological and Planetary Sciences, California Institute of Technology.



*Literature Cited*

Abe, Y., Matsui, T. 1985. The formation of an impact-generated $H_2O$ atmosphere and its implications for the early thermal history of the Earth. *Proc. Lunar Planet. Sci. Conf. 15th, Part 2, J. Geophys. Res.* 90: C545–59

Abe, Y., Matsui, T. 1986. Early evolution of the Earth: accretion, atmosphere formation and thermal history. *Proc. XVII Lunar Planet. Sci. Conf., I, J. Geophys. Res.* 91: E291–302

Abe, Y., Matsui, T. 1988. Evolution of an impact-generated $H_2O$-$CO_2$ atmosphere and formation of a hot proto-ocean on earth. *J. Atmos. Sci.* 45: 3081–3101

Ahrens, T. J. 1990. Earth accretion. In *Origin of the Earth*, ed. J. Jones, H. Newsom, pp. 211–27. Houston: Oxford Univ. Press

Ahrens, T. J., O'Keefe, J. D. 1987. Impact on the Earth, ocean, and atmosphere. *Proc. Hypervelocity Impact Symp., Int. J. Impact Eng.* 5: 13–32

Ahrens, T. J., O'Keefe, J. D., Lange, M. A. 1989. Formation of atmospheres during accretion of the terrestrial planets. In *Origin and Evolution of Planetary and Satellite Atmospheres*, ed. S. K. Atreya, J. B. Pollack, M. S. Matthews, pp. 328–85. Tucson: Univ. Ariz. Press

Allègre, C. J. 1982. Cosmochemistry and primitive evolution of planets. In *Formation of Planetary Systems*, ed. A. Brahic, pp. 283–364. Paris: Centre Natl. d'Etudes Spatiales

Arrhenius, G., De, B. R., Alfven, H. 1974. Origin of the ocean. In *The Sea*, ed. E. D. Goldberg, pp. 839–61. New York: Wiley

Bach, G. G., Kuhl, A. L., Oppenheim, A. K. 1975. On blast waves in exponential atmospheres. *J. Fluid Mech.* 71: 105–22

Båth, M. 1966. Earthquake energy and magnitude. *Phys. Chem. Earth* 7: 115–65

Beckwith, S., Sargent, A. I., Scoville, N. Z., Masson, C. R., Zuckerman, B., et al. 1986. Small-scale structure of the circumstellar gas of HL Tauri and R Monocerotis. *Astrophys. J.* 309: 755–61

Benlow, A., Meadows, A. J. 1977. The formation of the atmospheres of the terrestrial planets by impact. *Astrophys. Space Sci.* 46: 293–300

Benz, W., Cameron, A. G. W., Melosh, H. J. 1989. The origin of the moon and the single impact hypothesis, III. *Icarus* 81: 113–31

Benz, W., Slattery, W. L., Cameron, A. G. W. 1986. The origin of the moon and the single impact hypothesis, I. *Icarus* 66: 515–35

Benz, W., Slattery, W. L., Cameron, A. G. W. 1987. Origin of the moon and the single impact hypothesis, II. *Icarus* 71: 30–45

Benz, W., Slattery, W. L., Cameron, A. G. W. 1988. Collisional stripping of Mercury mantle. *Icarus* 74: 516–28

Cameron, A. G. W. 1983. Origin of the atmospheres of the terrestrial planets. *Icarus* 56: 195–201

Donahue, J. M., Hodges, R. R. Jr. 1992. Past and present water budget of Venus. *J. Geophys. Res.* 97: 6083–92

Duncan, M., Quinn, T., Tremaine, S. 1988. The origin of short-period comets. *Astrophys. J.* 328: 69–73

Goldreich, P., Ward, W. R. 1973. The formation of planetesimals. *Astrophys. J.* 183: 1051–61

Grinspoon, D. H., Lewis, J. S. 1988. Cometary water on Venus: implications for stochastic impacts. *Icarus* 74: 21–35

Hughes, H. G., App, F. N., McGetchen, T. R. 1977. Global effects of basin-forming impacts. *Phys. Earth Planet. Inter.* 15: 251–63

Hunten, D. M., Pepin, R. O., Owen, T. C. 1989. Planetary atmospheres. In *Meteor-*

*ites and the Early Solar System*, ed. J. F. Kerridge, M. S. Matthews, pp. 565–94. Tucson: Univ. Ariz. Press

Jessberger, E. K., Kissel, J., Rahe, J. 1989. The composition of comets. In *Origin and Evolution of Planetary Satellite Atmospheres*, ed. S. K. Atreya, J. B. Pollack, M. S. Matthews, pp. 167–91. Tucson: Univ. Ariz. Press

Jones, E. M., Kodis, J. W. 1982. Atmospheric effects of large body impacts; The first few minutes. In *Geological Implications of Impacts of Large Asteroids and Comets on the Earth*, ed. L. T. Silver, P. H. Schultz, pp. 175–86. Geol. Soc. Am. Spec. Pap.

Kanamori, H., Hauksson, E. 1992. A slow earthquake in the Santa Maria Basin, California. *Bull. Seismol. Soc. Am.* 82: 2087–96

Kaula, W. M. 1979. Thermal evolution of Earth and Moon growing by planetesimal impacts. *J. Geophys. Res.* 84: 999–1008

Kipp, M. E., Melosh, H. J. 1986. Short note: A preliminary study of colliding planets. In *Origin of the Moon*, ed. W. K. Hartmann, R. J. Phillips, G. T. Taylor, pp. 643–48. Houston: Lunar Planet. Inst.

Lange, M. A., Ahrens, T. J. 1982a. The evolution of an impact-generated atmosphere. *Icarus* 51: 96–120

Lange, M. A., Ahrens, T. J. 1982b. Impact-induced dehydration of serpentine and the evolution of planetary atmospheres. *Proc. Lunar Planet. Sci. Conf.* 13*th*, *Part* 1, *J. Geophys. Res., Suppl.* 87: A451–56

Levin, B. J. 1972. Origin of the earth. In *The Upper Mantle*, ed. A. R. Ritsema, pp. 7–30. Amsterdam: Elsevier

Matsui, T., Abe, Y. 1986a. Evolution of an impact-induced atmosphere and magma ocean on the accreting Earth. *Nature* 319: 303–5

Matsui, T., Abe, Y. 1986b. Impact induced atmospheres and oceans on Earth and Venus. *Nature* 322: 526–28

Melosh, H. J. 1989. *Impact Cratering, A Geologic Process*. New York: Oxford Univ. Press. 245 pp.

Melosh, H. J., Vickery, A. M. 1989. Impact erosion of the primordial Martian atmosphere. *Nature* 338: 487–89

Nakagawa, Y., Hayashi, C., Nakazawa, K. 1983. Accumulation of planetesimals in the solar nebula. *Icarus* 54: 361–76

O'Keefe, J. D., Ahrens, T. J. 1977a. Impact induced energy partitioning, melting, and vaporization on terrestrial planets. *Proc. Lunar Sci. Conf.*, 8*th*, Vol. 3, *Geochim. Cosmochim. Acta*, Suppl. 8: 3357–74

O'Keefe, J. D., Ahrens, T. J. 1977b. Meteorite impact ejecta: dependence on mass and energy lost on planetary escape velocity. *Science* 198: 1249–51

O'Keefe, J. D., Ahrens, T. J. 1982. The interaction of the Cretaceous-Tertiary extinction bolide with the atmosphere, ocean, and solid earth. *Geol. Soc. Am. Spec. Pap.* 190: 103–20

Owen, T., Bar-Nunn, A., Kleinfeld, I. 1992. Possible cometary origin of heavy noble gases in the atmospheres of Venus, Earth, and Mars. *Nature* 358: 43–45

Pollack, J. B., Bodenheimer, P. 1989. Theories of the origin and evolution of the giant planets. In *Origin and Evolution of Planetary and Satellite Atmospheres*, ed. S. K. Atreya, J. B. Pollack, M. S. Matthews, pp. 564–602. Tucson: Univ. Ariz. Press

Ringwood, A. E. 1979. *Origin of the Earth and Moon*. Berlin, New York: Springer-Verlag. 295 pp.

Safronov, V. S. 1969. *Evolution of the Proto-Planetary Cloud and Formation of the Earth and Planets*. Moscow: Nauka. Transl. for NASA and NSF by Isr. Prog. Sci. Transl. as NASA-TT-F677

Sargent, A. I., Beckwith, S. 1987. Kinematics of the circumstellar gas of HL Tauri and R Monocerotis. *Astrophys. J.* 323: 294–305

Sargent, A. I., Beckwith, S. V. 1991. The molecular structure around HL Tauri. *Astrophys. J. Lett.* 382: L31–35

Schultz, P. H., Gault, D. E. 1975. Seismically induced modification of lunar surface features. *Proc. Lunar Sci. Conf.* 6*th* 3: 2845–62

Shoemaker, W. M., Wolfe, R. F., Shoemaker, C. S. 1990. Asteroid and comet flux in the neighborhood of Earth. In *Global Catastrophes in Earth History*, ed. V. L. Sharpton, P. D. Ward, pp. 155–70. Geol. Soc. Am. Spec. Pap.

Smith, B. A., Terrile, R. J. 1984. A circumstellar disk around $\beta$-Pictoris. *Science* 226: 1421–24

Stewart, G. R., Kaula, W. M. 1980. Gravitational kinetic theory for planetesimals. *Icarus* 44: 154–71

Stewart, G. R., Wetherill, G. W. 1988. Evolution of planetesimal velocities. *Icarus* 74: 542–53

Vickery, A. M., Melosh, H. J. 1990. Atmospheric erosion and impactor retention in large impacts with application to mass extinctions. In *Global Catastrophes in Earth History*, ed. V. L. Sharpton, P. O. Ward, pp. 289–300. Geol. Soc. Am. Spec. Pap.

Walker, J. C. G. 1986. Impact erosion of planetary atmospheres. *Icarus* 68: 87–98

Watts, A. W., Greeley, R., Melosh, H. J. 1991. The formation of terrains antipodal to major impacts, *Icarus* 93: 159–68

Weidenschilling, S. J. 1988. Formation processes and time scales for meteorite parent bodies. In *Meteorites and the Early Solar System*, ed. J. F. Kerridge, M. S. Matthews, pp. 348–71. Tucson: Univ. Ariz. Press

Weidenschilling, S. J., Donn, B., Meakin, P. 1989. Physics of planetesimal formation. In *The Formation and Evolution of Planetary Systems*, ed. H. A. Weaver, L. Danly, pp. 131–50. Cambridge: Cambridge Univ. Press

Wetherill, G. W. 1980. Formation of the terrestrial planets. *Annu. Rev. Astron. Astrophys.* 18: 77–113

Wetherill, G. W. 1990. Formation of the Earth. *Annu. Rev. Earth Planet. Sci.* 18: 205–56

Zahnle, K. J., Kasting, J. F., Pollack, J. B. 1988. Evolution of a steam atmosphere during Earth's accretion. *Icarus* 74: 62–97

Zahnle, K., Pollack, J. B., Grinspoon, D. 1992. Impact-generated atmospheres over Titan, Ganymede, and Callisto. *Icarus* 95: 1–23

Zel'dovich, Y. B., Raizer, Y. P. 1966. *Physics of Shock Waves and High-Temperature Hydrodynamic Phenomena*. Vol. 112. New York: Academic. 916 pp.

*Annual Review of Earth and Planetary Sciences*
*Volume 21, 1993*

# CONTENTS